JÖNSEN, P.-G. & OLOVSSON, I. (1968). *Acta Cryst.* B**24**, 559–564.
KOJIĆ-PRODIĆ, B., MATKOVIC, B. & SCAVNICAR, S. (1971). *Acta Cryst.* B**27**, 635–637.
KOJIĆ-PRODIĆ, B., SCAVNICAR, S. & MATKOVIC, B. (1971). *Acta Cryst.* B**27**, 638–644.
KRONBERG, M. L. & HARKER, D. (1942). *J. Chem. Phys.* **10**, 309–317.
LOOPSTRA, L. H. & MACGILLAVRY, C. (1958). *Acta Cryst.* **11**, 349–354.
LUNDGREN, J. O. & OLOVSSON, I. (1976). In *The Hydrogen Bond*, edited by P. SCHUSTER, G. ZUNDEL & C. SANDORFY, Amsterdam, New York, Oxford: North Holland.
MAARTMANN-MOE, K. (1969). *Acta Cryst.* B**25**, 1452–1460.
MCDONALD, T. R. R. (1960). *Acta Cryst.* **13**, 113–124.
MONTGOMERY, H. (1980). *Acta Cryst.* B**36**, 2121–2123.
MOROSIN, B. (1970). *Acta Cryst.* B**26**, 1635–1637.
NELMES, R. J. (1971). *Acta Cryst.* B**27**, 272–281.
OTTERSEN, T., CHRISTOPHERSEN, C. & TREPPENDAHL, S. (1975). *Acta Chem. Scand Ser. A*, **29**, 45–50.
OWSTON, P. G., SHAW (NÉE GÖZEN), L. S. & TASKER, P. A. (1982). *J. Chem. Soc. Chem. Commun.* pp. 17–19.
PASCARD-BILLY, C. (1965). *Acta Cryst.* **18**, 827–829.
PRINGLE, G. E. & BROADBENT, T. A. (1965). *Acta Cryst.* **19**, 426–432.
ROGERS, R. D., KURIHARA, L. K. & RICHARDS, P. D. (1987). *J. Chem. Soc. Chem. Commun.* pp. 604–606.
SCHAEFER, W. P., EALICK, S. E. & MARSH, R. E. (1981). *Acta Cryst.* B**37**, 34–38.
SCHAEFER, W. P. & MARSH, R. E. (1966). *Acta Cryst.* **21**, 735–743.
SCHLEMPER, E. O., HAMILTON, W. C. & RUSH, J. J. (1966). *J. Chem. Phys.* **44**, 2499–2505.
SEIDEL, F. (1926). *Ber. Dtsch. Chem. Ges.* **60**, 1894–1908.
SEIDEL, F. & DICK, S. (1927). *Ber. Dtsch. Chem. Ges.* **60**, 2018–2023.
SHELDRICK, G. M. (1976). *SHELX*76. Program for crystal structure determination. Univ. of Cambridge, England.
SHELDRICK, G. M. & TROTTER, J. (1978). *Acta Cryst.* B**34**, 3122–3124.
SKURATOWICZ, J. S., MADDEN, I. L. & BUSCH, D. H. (1977). *Inorg. Chem.* **16**, 1721–1725.
SONNEVELD, E. J. & VISSER, J. W. (1978). *Acta Cryst.* B**34**, 643–645.
SONNEVELD, E. J. & VISSER, J. W. (1979). *Acta Cryst.* B**35**, 1975–1977.
STEWART, R. F., DAVIDSON, E. R. & SIMPSON, W. T. (1965). *J. Chem. Phys.* **42**, 3175–3187.
SUTOR, D. J. (1962). *Nature (London)*, **195**, 68–69.
SUTOR, D. J. (1963). *J. Chem. Soc.* pp. 1105–1110.
SUZUKI, S. & MAKITA, Y. (1978). *Acta Cryst.* B**34**, 732–735.
TAESLER, I. & OLOVSSON, I. (1968). *Acta Cryst.* B**24**, 299–304.
TAYLOR, R. & KENNARD, O. (1982). *J. Am. Chem. Soc.* **104**, 5063–5070.
THEWALT, U. & BUGG, C. E. (1972). *Acta Cryst.* B**28**, 82–92.
TUCKER, P. A., HOEKSTRA, A., TEN CATE, J. M. & VOS, A. (1975). *Acta Cryst.* B**31**, 733–737.

Acta Cryst. (1988). B**44**, 50–55

Experimental Electron Density Distribution of (1*R**,2*S**,3*R**,4*R**)-3,4-Epoxy-1,2,3,4-tetrahydro-1,2-naphthalenediol

BY CHERYL L. KLEIN

Department of Chemistry, Xavier University of Louisiana, New Orleans, Louisiana 70125, *USA*

AND EDWIN D. STEVENS

Department of Chemistry, University of New Orleans, New Orleans, Louisiana 70148, *USA*

(*Received* 25 *February* 1986; *accepted* 12 *August* 1987)

Abstract

Careful X-ray diffraction measurements at 100 K have been used to map the electron density distribution in a single crystal of *trans*-3,4-epoxy-1,2,3,4-tetrahydro-1,2-naphthalenediol, a small-molecule model for the ultimate carcinogenic metabolites of some polycyclic aromatic hydrocarbons. A least-squares-refinement procedure has been used in which additional multipole parameters are added to describe the distortions of the atomic electron distributions as a result of covalent bonding. The refinement also yields improved estimates of the X-ray phases, which have been used to plot maps of the electron distribution. In the epoxide ring, one C atom is found to be more positive than the other, suggesting that it would be the preferred site of attack by nucleophiles such as DNA bases, in agreement with other experimental evidence. Covalent-bond peaks lie outside the lines joining the atom centers of the epoxide ring, and lone-pair density on the epoxide O atom corresponds to largely unhybridized *s* and *p* orbitals. Crystal data: $C_{10}H_{10}O_3$, $M_r = 178{\cdot}0$, space group $Pna2_1$, $a = 7{\cdot}979\ (2)$, $b = 8{\cdot}634\ (3)$, $c = 23{\cdot}560\ (5)$ Å, $V = 1623{\cdot}1\ (8)$ Å^3, $Z = 8$, $D_x = 1{\cdot}46$ g cm^{-3}, Mo $K\alpha$ radiation, $\lambda = 0{\cdot}70930$ Å, $\mu = 1{\cdot}16$ cm^{-1}, $F(000) = 752$, $T = 105$ K, $R = 0{\cdot}058$ for 2575 observed reflections for the multipole refinement.

Introduction

Many polycyclic aromatic hydrocarbons, such as benzo[*a*]pyrene, are known to be common environmental pollutants and potent chemical carcinogens. Several

0108-7681/88/010050-06$03.00

metabolic derivatives of these hydrocarbons result from successive enzymatic oxidation by mixed-function oxygenase enzymes and hydrolysis reactions (Harvey, 1981, 1982). The ultimate carcinogenic metabolite of many polyaromatic hydrocarbons is believed to be the diol epoxide of the parent hydrocarbon (Sims, Grover, Swaisland, Pal & Hewer, 1974).

In recent years, experimental techniques have been developed to measure directly the electron distributions of molecules using accurate high-resolution X-ray diffraction data (Coppens & Hall, 1982; Coppens & Stevens, 1977). In this study, we investigate the possibility that experimental electron distributions may yield not only information on the electronic structures of chemical carcinogens and their metabolites, but may also be useful in predicting sites of chemical attack in the various steps involved in carcinogenesis. For example, the sites of electrophilic attack in the metabolic activation of polycyclic aromatic hydrocarbons may be predictable from experimental electron density distributions of the parent hydrocarbons. In addition, since the mode of interaction of a metabolite with DNA and other cellular targets will certainly be dependent on the electronic character as well as the stereochemistry of the molecule involved, the sites of reaction on the metabolite may be predictable from high-resolution studies.

We report here the results of the experimental electron density mapping of the title compound (hereafter referred to as naphthalene diol epoxide, NDE), a small-molecule model for the ultimate carcinogenic metabolite of benzo[*a*]pyrene and other polyaromatic hydrocarbons. The structure of NDE has been determined previously at room temperature (Klein & Stevens, 1984).

Experimental

Data collection

NDE was prepared as described previously (Tsang, Griffin, Horning & Stillwell, 1982). Despite numerous attempts in many different solvents, crystals inevitably grew as thin needles. Crystals for data collection were grown by evaporation of an ethyl acetate solution. A single colorless crystal with dimensions 0·15 × 0·15 × 0·7 mm was mounted on an Enraf–Nonius CAD-4 diffractometer and cooled to 100 K with a stream of cold nitrogen gas. Unit-cell dimensions were obtained by least-squares refinement of 25 reflections with $36{\cdot}5 \leq 2\theta \leq 54°$.

X-ray intensity measurements were collected in the $\theta/2\theta$ scan mode with a graphite-crystal monochromator and Mo $K\alpha$ radiation. Because of the large value of one of the crystal dimensions, a standard-focus X-ray tube and 1·3 mm incident-beam collimator were used, yielding an incident beam measured to be uniform (±2%) within a diameter of 0·9 mm. Scan speeds were adjusted according to the intensity measured during a fast prescan, resulting in scan times of between 30 and 600 s per reflection. 12 438 reflections were collected from four symmetry-equivalent octants to a 2θ maximum of 80° [$(\sin\theta_{max})/\lambda = 0{\cdot}9$ Å^{-1}]. The data were corrected for Lorentz and polarization effects. Absorption as a function of ψ was corrected empirically (minimum transmission factor 0·93; maximum transmission factor 0·99). Three standard reflections measured at 2 h intervals showed only minimal fluctuation of ±0·3%. Equivalent symmetry-related reflection intensities were averaged in order to lower the standard deviations in the measurements. The final data set gave 5106 independent reflections with internal agreement factors of $R(F^2) = 4{\cdot}2\%$ and $wR(F^2) = 5{\cdot}7\%$ for all observations.

Least-squares refinements

The quantity $\sum w(|kF_o| - |F_c|)^2$ with $w = 1/\sigma(F)^2$ was minimized by full-matrix least-squares refinement. $\sigma(F)^2$ was taken as $[\sigma(F)^2_{cs} + (0{\cdot}03F^2)^2]$ where σ_{cs} represents the contribution from counting statistics. Because of the crystal size, many of the reflections were weak. To provide an adequate ratio of observations to parameters, only reflections where F_o was less than $1{\cdot}5\sigma(F)$ were considered unobserved and were not included in the refinement. Since this low cutoff leads to the higher R factors, agreement factors based on those reflections with $F_o > 3\sigma$ were also calculated. Computer programs used for data collection, reduction and conventional refinements are part of the CAD-4 *SDP* package (Frenz, 1982). Scattering factors were taken from *International Tables for X-ray Crystallography* (1974) and included corrections for anomalous-scattering contributions in the O- and C-atom scattering-factor tables.

To reduce bias in refined parameters from the aspherical features of the valence electron density, the parameters were refined using only high-angle data [$(\sin\theta)/\lambda > 0{\cdot}65$ Å^{-1}] for which the scattering is due mainly to the core electrons. H-atom coordinates were obtained by extending the located H-atom positions along the bond to positions yielding C—H and O—H bond distances typical of values determined by neutron diffraction experiments. Isotropic thermal parameters of the H atoms were fixed at the values obtained in the full-data refinement.

An alternative technique for avoiding bias in the refined parameters is to include additional variables in the least-squares refinement which describe the aspherical features of the valence density (Dawson, 1967; Harel & Hirshfeld, 1975; Stewart, 1976). In the model used here (Hansen & Coppens, 1978), deformations of the electron density at each atom are

described by an expansion of multipole density functions

$$\rho_{\text{atom}} = \rho_c(r) + P_v\rho_v(\kappa' r) + \sum_{l,m} P_{l,m} R_l(\kappa'' r) y_{l,m}(\theta,\varphi),$$

where ρ_c and ρ_v are spherical Hartree–Fock core and valence densities and the $y_{l,m}$ are spherical harmonic functions in real form. The radial functions are given by

$$R_l(r) = Nr^n \exp(-\zeta r),$$

where n and ζ are chosen for each l as described previously (Hansen & Coppens, 1978; Stevens, 1981). The P_v, $P_{l,m}$, κ' and κ'' are refinable parameters. Positional and thermal parameters for H atoms were obtained in the same manner as the high-order refinement and fixed at those values. The results of the various refinements are summarized in Table 1.*

Table 1. *Refinement results*

	I*	II†	III‡
$(\sin\theta)/\lambda$ range (Å^{-1})	0·0–0·90	0·65–0·90	0·0–0·90
For all 2575 reflections included in the refinement			
R	0·074	0·090	0·058
wR	0·058	0·085	0·044
S	1·44	1·13	0·93
N_{obs}	2575	1052	2575
N_v	314	234	389
For reflections with $F_o > 3\sigma$			
R	0·054	0·070	0·038
wR	0·053	0·073	0·036
S	1·56	1·24	0·99
N_{obs}	1902	780	1902

* Conventional full data refinement.
† High-order refinement.
‡ Multipole refinement.

Electron density maps

Distortions of the atomic electron distributions in a molecule as a result of chemical bonding are revealed in a plot of the deformation density, $\Delta\rho$, given as the difference between the total observed density and the density calculated for a superposition of spherical neutral Hartree–Fock atoms. Since the space group of NDE is noncentrosymmetric the experimental $\Delta\rho_{HO}$ deformation densities suffer from the fact that only the amplitude and not the phase of the structure factor can be determined from the X-ray experiment. This has the effect of reducing the height and smearing out the features in the deformation density map (Savariault & Lehmann, 1980; Stevens, 1981).

The maps presented here are dynamic model deformation density maps where both the amplitude and the phase of the structure factors used to calculate the maps are those obtained from the multipole refinement (Stevens, 1981). In order to avoid errors in the Fourier summation due to missing reflections, all unique reflections have been calculated and included up to a resolution of $(\sin\theta)/\lambda = 1{\cdot}0$ Å^{-1}.

On the basis of the errors in the X-ray measurements, the average standard deviation in the deformation density maps is estimated to be 0·05 e Å^{-3}. Close to the atom centers, however, because the deformation density is the difference between large values of the electron density, uncertainty in the scale factor and the positional and thermal parameters of the atoms will lead to much larger e.s.d.'s.

Residual maps, calculated by a difference Fourier summation between the observed and multipole structure factors, show no features greater than three times the e.s.d. This confirms the validity of the constraint that the density in the two independent molecules be identical, and the additional local symmetry constraints placed on the multipole deformation parameters.

Results and discussion

Specific structural characteristics for NDE based on low-order room-temperature data have been described previously (Klein & Stevens, 1984). Fig. 1 is an *ORTEP* (Johnson, 1965) diagram which shows the structure and the numbering system for one of the two molecules in the asymmetric molecular unit. In the multipole refinement of the electron density, the parameters that describe the distribution of electrons for the two unique molecules were constrained to be the same. Therefore, the model deformation density map, shown in Fig. 2, would have exactly the same density features as the other molecule. Fig. 2 shows the deformation density calculated in the plane of the molecule. In the center of each bond in the ring, there are peaks of electron density which correspond to the covalent bonds that result from the sharing of electrons. On each of the atom positions, there is a slight hole where the atomic electron density has been subtracted. Dotted contours correspond to negative areas of electron density and solid contours correspond to positive areas of electron density. The saturated ring in the molecule can be described as having a twist-boat conformation. The plane defined by the aromatic ring does not pass through all of the atoms in the saturated portion of the molecule. As a result, the calculated electron density in this plane will not show density in all of the bonds. Fig. 2 was therefore generated by taking a composite of the density calculated in planes defined by groups of three atoms in the rings.

Fig. 3 shows a model deformation density map for two hydroxyl groups and their hydrogen-bond network.

* Tables of atom positions, thermal parameters, refined multipole radial and population parameters, and structure-factor amplitudes have been deposited with the British Library Document Supply Centre as Supplementary Publication No. SUP 44274 (26 pp.). Copies may be obtained through The Executive Secretary, International Union of Crystallography, 5 Abbey Square, Chester CH1 2HU, England.

Each hydroxyl O atom participates in two hydrogen bonds (shown with dashed lines). In one hydrogen bond, O(2) donates its hydrogen, HY(2), into the hydrogen bond formed with O(3) from an adjacent molecule. O(2) also accepts a hydrogen atom, HY(3), from a different adjacent molecule to form a second hydrogen bond. Although not obvious from the figure, which shows the density in only one plane, the hydrogen bonds are directed towards the oxygen lone pairs rather than toward the oxygen centers. One should notice also that there is no electron density in the center of the hydrogen bond as expected for long hydrogen bonds since the formation of these types of interactions result primarily from electrostatic attraction with little covalent contribution.

Of greatest interest is the electron distribution in the epoxide ring, since this is the functional group believed to be responsible for the reactivity of diol epoxide metabolites of carcinogenic hydrocarbons. Although it has no 'bay' region and fewer aromatic rings, NDE is structurally similar in the epoxide-ring regions to the corresponding regions of other polyaromatic hydrocarbon oxides [5,6-epoxy-7,12-dimethylbenzanthracene and 9,10-epoxyphenanthrene (Glusker, Carrell, Zacharias & Harvey, 1974), 4,5-epoxybenzo[*a*]pyrene (Glusker, Zacharias, Carrell, Fu & Harvey, 1976) and especially 9β,10β-epoxy-7,8,9,10-tetrahydrobenzo[*a*]-pyrene-7α,8β-diol, BPDE (Neidle, Subbiah, Cooper & Robeiro, 1980)]. Fig. 4 shows the deformation density calculated through the epoxide-ring plane. At the center of the ring, the contours decrease in height to form a local minimum in the middle of the ring. Since

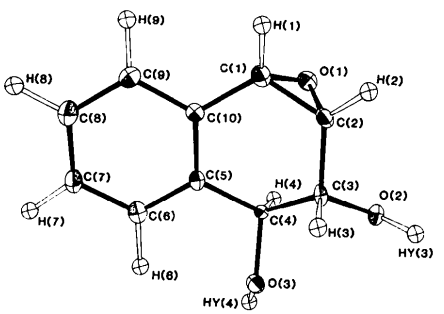

Fig. 1. Atomic labeling scheme and molecular structure in one molecular unit of naphthalene diol epoxide. The thermal ellipsoids are plotted at the 50% probability level.

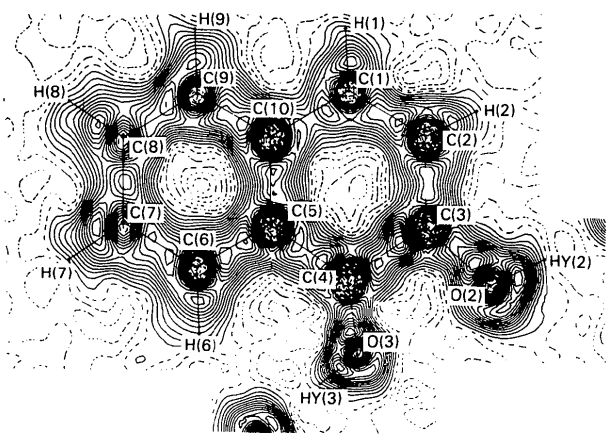

Fig. 2. Model deformation density map of naphthalene diol epoxide in the plane of the molecule. In the saturated ring, the map represents a composite of planes calculated through the bonds. Contours are at 0·10 e Å^{-3} intervals with the zero and negative contours dashed.

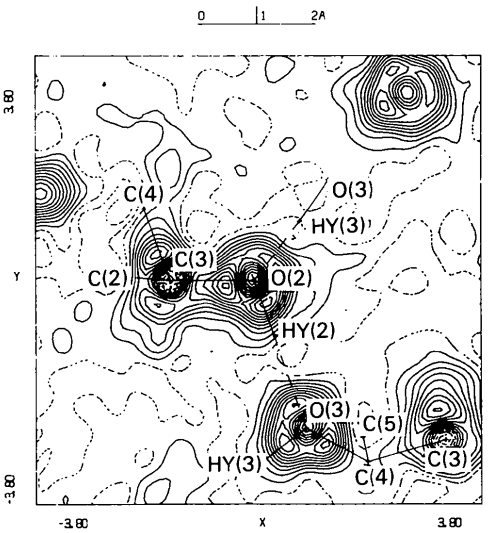

Fig. 3. Model deformation density map calculated in the plane defined by C(3), O(2) and O(3′) showing the O(2)–HY(2)···O(3′) hydrogen-bond density. Hydrogen bonds are shown with dashed lines. Contours are plotted at 0·07 e Å^{-3} intervals.

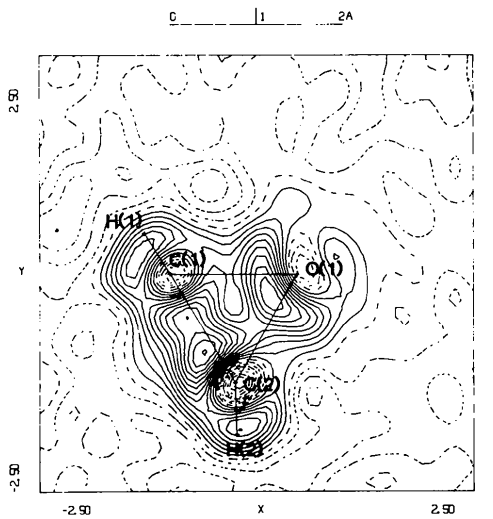

Fig. 4. Model deformation density map calculated in the plane of the epoxide ring. Contours are plotted at 0·05 e Å^{-3} intervals.

three-membered rings are highly strained systems, 'bent' bonds are expected between atoms. This is evident in the deformation density maps by the location of the C(1)–C(2) covalent-bond peak outside the straight line drawn to connect the atom centers. The C–O bond peaks are polarized toward the more electronegative O atom; and, at the resolution of this study, the C–O bond peaks merge into a single peak inside the ring. Careful tracing of the bond paths, however, also suggests bent bonding for the C–O bonds.

Fig. 5 shows the density calculated in a plane perpendicular to the C(1)–C(2) bond of the epoxide ring and passing through the epoxide O atom. The nonbonded 'lone-pair' density on the O atom is clearly evident and appears to possess predominantly *p* character. This phenomenon is supported by examination of the molecular-orbital coefficients of an *ab initio* theoretical calculation on oxirane (Politzer & Daiker, 1977) which indicate largely unhybridized *s* and *p* lone pairs on the O atom.

The electron density in the C–O bonds in the epoxide ring appears to be polarized toward the O atom (Fig. 4). This is a common feature in bonds that contain one atom that is more electronegative than the other. The C(1)–C(2) bond also shows an asymmetric electron density where the density is polarized towards C(2). This asymmetry is confirmed by the magnitude of the monopole populations which shows that C(2) is significantly more negative than C(1) [net atomic charges: C(1) = +0·37 and C(2) = −1·38, with e.s.d.'s of 0·38 and 0·53 respectively – the high e.s.d.'s reflect the well known difficulty of partitioning a continuous electron distribution into atomic fragments]. From this information the site of chemical attack by a nucleophile on the epoxide ring can be predicted. Aside from steric consideration, attack by a nucleophile is expected at C(1), the most electropositive atom of the epoxide ring in NDE. The reaction of epoxide metabolites of polyaromatic hydrocarbons such as BPDE with DNA has been shown to result in adducts in which the carcinogen is covalently bound to DNA bases, predominantly at guanosine (Jeffrey, Jennette, Blobstein, Weinstein, Beland, Harvey, Kasai, Miura & Nakanishi, 1976; Weinstein, Jeffrey, Jennette, Blobstein, Harvey, Kasai & Nakanishi, 1976). Such a reaction, which can be considered as a nucleophilic attack by the DNA base, has been shown to occur at a C atom equivalent to the C(1) atom of NDE both for BPDE (Jeffrey *et al.*, 1976) and the *trans*-8,9-diol 10,11-epoxide of benz[*a*]anthracene (Cary, Turner, Copper, Robeiro, Grover & Sims, 1980). While the specific stereochemistry of the interaction of the ultimate carcinogen with the DNA molecule must also be important, the electron distribution observed in NDE is consistent in predicting the reaction sites found for both bay-region and non-bay-region epoxides.

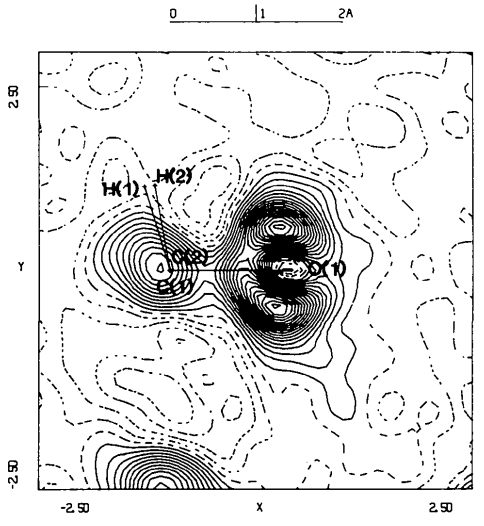

Fig. 5. Model deformation density map calculated in a plane perpendicular to the C(1)–C(2) bond of the epoxide ring which passes through the epoxide O atom. Contours are at 0·05 e Å^{-3} intervals.

The experimental electron density distribution provides a very detailed function which can be used for the calibration of theoretical calculations. Another property of the electron distribution which has been developed by theoretical chemists for predicting chemical reactivities is the electrostatic potential (Politzer, Trefonas, Politzer & Elfman, 1981). However, this is a property which can also be obtained experimentally from the X-ray-determined electron distribution. We believe that extension of these studies to the metabolites of carcinogenic polyaromatic hydrocarbons will provide useful information on the electronic characteristics and reactivity of these intermediates. For example, comparison of the result on NDE reported here with experimental electron densities of a bay-region diol epoxide will show any effects of the bay region on the electronic structure of the molecule. Studies of the parent hydrocarbons should also be of value in predicting sites of reaction by electrophilic oxygen of mixed-function oxidases in the initial steps of metabolism.

We thank the Cancer Association of Greater New Orleans for partial support of this work.

References

CARY, P. D., TURNER, C. H., COOPER, G. S., ROBEIRO, O., GROVER, P. L. & SIMS, P. (1980). *Carcinogenesis*, **1**, 505–512.

COPPENS, P. & HALL, M. B. (1982). *Electron Distributions and the Chemical Bond*. New York: Plenum.

COPPENS, P. & STEVENS, E. D. (1977). *Adv. Quantum Chem.* **10**, 1–35.

DAWSON, B. (1967). *Proc. R. Soc. London Ser. A*, **298**, 255–263.

FRENZ, B. (1982). *Computing in Crystallography*, edited by H. SCHENK, R. OLTHHOF-HAZEKAMP, H. VAN KONINGSVELD & G. C. BASSI. Delft Univ. Press.
GLUSKER, J. P., CARRELL, H. L., ZACHARIAS, D. E. & HARVEY, R. G. (1974). *Cancer Biochem. Biophys.* **1**, 43–52.
GLUSKER, J. P., ZACHARIAS, D. E., CARRELL, H., FU, P. P. & HARVEY, R. G. (1976). *Cancer Res.* **36**, 3951–3957.
HANSEN, N. K. & COPPENS, P. (1978). *Acta Cryst.* A**34**, 909–921.
HAREL, M. & HIRSHFELD, F. L. (1975). *Acta Cryst.* B**31**, 162–172.
HARVEY, R. G. (1981). *Acc. Chem. Res.* **14**, 218–226.
HARVEY, R. G. (1982). *Am. Sci.* **70**, 386–393.
International Tables for X-ray Crystallography (1974). Vol. IV. Birmingham: Kynoch Press. (Present distributor D. Reidel, Dordrecht.)
JEFFREY, A. M., JENNETTE, K. W., BLOBSTEIN, S. H., WEINSTEIN, I. B., BELAND, P., HARVEY, R. G., KASAI, H., MIURA, I. & NAKANISHI, K. (1976). *J. Am. Chem. Soc.* **98**, 5714–5715.
JOHNSON, C. K. (1965). *ORTEP*. Report ORNL-3794. Oak Ridge National Laboratory, Oak Ridge, Tennessee, USA.
KLEIN, C. L. & STEVENS, E. D. (1984). *Cancer Res.* **44**, 1523–1526.
NEIDLE, S., SUBBIAH, A., COOPER, C. S. & ROBEIRO, O. (1980). *Carcinogenesis*, **1**, 249–254.
POLITZER, P. & DAIKER, K. C. (1977). *Int. J. Quantum. Chem. Symp.* **4**, 317–325.
POLITZER, P., TREFONAS, P., POLITZER, I. R. & ELFMAN, B. (1981). *Ann. N. Y. Acad. Sci.* **367**, 478–492.
SAVARIAULT, J.-M. & LEHMANN, M. S. (1980). *J. Am. Chem. Soc.* **102**, 1298–1303.
SIMS, P., GROVER, P. L., SWAISLAND, A., PAL, K. & HEWER, A. (1974). *Nature (London)*, **252**, 326–327.
STEVENS, E. D. (1981). *J. Am. Chem. Soc.* **103**, 5087–5095.
STEWART, R. F. (1976). *Acta Cryst.* A**32**, 565–574.
TSANG, W.-S., GRIFFIN, G. W., HORNING, M. G. & STILLWELL, W. G. (1982). *J. Org. Chem.* **47**, 5339–5353.
WEINSTEIN, I. B., JEFFREY, A. M., JENNETTE, K. W., BLOBSTEIN, S. H., HARVEY, R. G., KASAI, H. & NAKANISHI, K. (1976). *Science*, **193**, 592–595.

Acta Cryst. (1988). B**44**, 55–63

Charge-Transfer Complexes of Hydrazones. VI.* Structures of Six Hydrazone Derivatives. Infrared and Structural Evidence for Substituent Effects on Charge-Transfer Interactions

BY GIORGIO TOSI† AND LIBERATO CARDELLINI

Dipartimento di Scienze dei Materiali, Facoltà di Ingegneria, Università di Ancona, Via Brecce Bianche, I-60131, Ancona, Italy

AND GABRIELE BOCELLI

Centro di Studio per la Strutturistica Diffrattometrica del CNR, Viale delle Scienze, I-43100, Parma, Italy

(*Received* 11 *December* 1986; *accepted* 15 *September* 1987)

Abstract

The problems connected with the formation of charge-transfer complexes were examined by analysis of the IR spectra of 21 phenylhydrazones and determination of the crystal structures of six of them at room temperature with Cu $K\alpha$ radiation ($\lambda = 1.5418$ Å). Benzaldehyde methyl(phenyl)hydrazone (compound 2): $C_{14}H_{14}N_2$, $M_r = 210.3$, monoclinic, $P2_1/a$, $a = 22.896$ (2), $b = 9.201$ (2), $c = 5.559$ (2) Å, $\beta = 91.53$ (3)°, $V = 1170.7$ (5) Å^3, $Z = 4$, $D_x = 1.19$ g cm^{-3}, $\mu = 5.19$ cm^{-1}, $F(000) = 448$, the final R was 0.055 for 709 observed reflections. Acetophenone methyl(phenyl)hydrazone (compound 5): $C_{15}H_{16}N_2$, $M_r = 224.3$, orthorhombic, $P2_12_12_1$, $a = 20.099$ (3), $b = 8.644$ (2), $c = 7.537$ (2) Å, $V = 1309.5$ (5) Å^3, $Z = 4$, $D_x = 1.14$ g cm^{-3}, $\mu = 4.90$ cm^{-1}, $F(000) = 480$, the final R was 0.051 for 921 observed reflections. Benzophenone methyl(phenyl)hydrazone (compound 8): $C_{20}H_{18}N_2$, $M_r = 286.4$, monoclinic, $P2_1/n$, $a = 16.122$ (2), $b = 10.482$ (2), $c = 9.586$ (2) Å, $\beta = 92.35$ (3)°, $V = 1618.6$ (5) Å^3, $Z = 4$, $D_x = 1.17$ g cm^{-3}, $\mu = 5.01$ cm^{-1}, $F(000) = 608$, the final R was 0.044 for 1584 observed reflections. Benzophenone diphenylhydrazone (compound 9): $C_{25}H_{20}N_2$, $M_r = 348.4$, monoclinic, $P2_1/n$, $a = 12.355$ (2), $b = 13.741$ (3), $c = 11.543$ (2) Å, $\beta = 96.13$ (2)°, $V = 1948.5$ (6) Å^3, $Z = 4$, $D_x = 1.19$ g cm^{-3}, $\mu = 5.03$ cm^{-1}, $F(000) = 736$, the final R was 0.043 for 2761 observed reflections. *p*-Methoxybenzaldehyde methyl(phenyl)hydrazone (compound 11): $C_{15}H_{16}N_2O$, $M_r = 240.3$, orthorhombic, $P2_12_12_1$, $a = 25.980$ (3), $b = 9.017$ (2), $c = 5.606$ (2) Å, $V = 1313.3$ (6) Å^3, $Z = 4$, $D_x = 1.22$ g cm^{-3}, $\mu = 5.78$ cm^{-1}, $F(000) = 512$, the final R was 0.041 for 826 observed reflections. 2-Nitrobenzaldehyde methyl(phenyl)hydrazone (compound 12): $C_{14}H_{13}N_3O_2$, $M_r = 255.3$, monoclinic, $P2_1/a$, $a = 18.567$ (2), $b = 8.109$ (2), $c = 8.592$ (1) Å, $\beta = 94.09$ (2)°, $V = 1290.3$ (4) Å^3, $Z = 4$, $D_x = 1.31$ g cm^{-3}, $\mu = 7.04$ cm^{-1}, $F(000) = 536$, the final R

* Part V: Bruni, Tosi & Cardellini (1988).

† To whom correspondence should be addressed.

0108-7681/88/010055-09$03.00